JOURNAL OF THE AMERICAN CHEMICAL SOCIETY

Subscriber access provided by Bibliothèque de l'Université Paris-Sud

Communication

Synergistic Cu Catalysts for Formic Acid Dehydrogenation

Takayuki Nakajima, Yoshia Kamiryo, Masayo Kishimoto, Kaho
Imai, Kanako Nakamae, Yasuyuki Ura, and Tomoaki Tanase

J. Am. Chem. Soc., **Just Accepted Manuscript** • DOI: 10.1021/jacs.9b03532 • Publication Date (Web): 14 May 2019

Downloaded from http://pubs.acs.org on May 14, 2019

Just Accepted

"Just Accepted" manuscripts have been peer-reviewed and accepted for publication. They are posted online prior to technical editing, formatting for publication and author proofing. The American Chemical Society provides "Just Accepted" as a service to the research community to expedite the dissemination of scientific material as soon as possible after acceptance. "Just Accepted" manuscripts appear in full in PDF format accompanied by an HTML abstract. "Just Accepted" manuscripts have been fully peer reviewed, but should not be considered the official version of record. They are citable by the Digital Object Identifier (DOI®). "Just Accepted" is an optional service offered to authors. Therefore, the "Just Accepted" Web site may not include all articles that will be published in the journal. After a manuscript is technically edited and formatted, it will be removed from the "Just Accepted" Web site and published as an ASAP article. Note that technical editing may introduce minor changes to the manuscript text and/or graphics which could affect content, and all legal disclaimers and ethical guidelines that apply to the journal pertain. ACS cannot be held responsible for errors or consequences arising from the use of information contained in these "Just Accepted" manuscripts.

ACS Publications

is published by the American Chemical Society. 1155 Sixteenth Street N.W.,
Washington, DC 20036

Published by American Chemical Society. Copyright © American Chemical Society.
However, no copyright claim is made to original U.S. Government works, or works
produced by employees of any Commonwealth realm Crown government in the course
of their duties.

Synergistic Cu$_2$ Catalysts for Formic Acid Dehydrogenation

Takayuki Nakajima*, Yoshia Kamiryo, Masayo Kishimoto, Kaho Imai, Kanako Nakamae, Yasuyuki Ura, Tomoaki Tanase*

Department of Chemistry, Faculty of Science, Nara Women's University, Kitauoya-nishi-machi, Nara 630-8506, Japan

Supporting Information Placeholder

ABSTRACT: Hexanuclear copper hydride complexes, [Cu$_6$(μ_3–H)$_2$(*meso*–**L**^{4})$_3$(RNC)$_4$](PF$_6$)$_4$ (R = ^{t}Bu (**6a**), Cy (**6b**)), were prepared by using a new linear tetraphosphine, *meso*–Ph$_2$PCH$_2$P(Ph)(CH$_2$)$_4$P(Ph)CH$_2$PPh$_2$ (*meso*–**L**^{4}), and were converted into active catalysts of [Cu$_2$(μ–O$_2$CH)(*meso*–**L**^{4})(RNC)$_2$]$^+$ under the reaction conditions of FA dehydrogenation, where unsymmetric dinuclear copper sites supported by the tetradentate phosphine and isocyanide ligands were essential to demonstrate effective catalytic activity.

Hydrogen gas is one of the best promising energy carriers, if it is green, since it can be storable and used on demand to complement intermittent energy gaps with an aim of constructing sustainable energy systems with minimizing environmental impacts. From a view point of storing and transporting H$_2$ gas efficiently as non-hazardous material, formic acid (FA) has been considered as a viable hydrogen carrier, and hence, its decomposition into H$_2$ and CO$_2$ has been extensively studied as well as hydrogenation of CO$_2$ into FA.[1] While noble metal homogeneous catalysts based on Ru, Rh, and Ir have widely been investigated,[1] non-noble base metallic systems except for Fe and Ni [1] are yet to be studied, and in particular, selective decomposition of FA by Cu based systems is still largely unexplored; only very poor catalytic activity was reported with Cu(OAc)$_2$ and Et$_3$N combination[2] although gas-phase FA decomposition was recently reported.[3] For the past a couple of decades, copper hydride species have attracted considerable interest due to their application for the chemoselective reductions of unsaturated organic compounds including CO$_2$.[4,5] The reactivity and selectivity are manipulated by the nature of the copper hydride intermediates, which have originally been supported by monophosphine ligands.[6] In recent years, however, with an aim of establishing synergistic reactivity arising from multinuclear Cu–H species, several groups have reported syntheses of Cu–H complexes supported by di- and tridentate phosphine ligands, such as 1,2-bis(diphenylphosphino)benzene (dppbz), bis(diphenylphosphino)methane (dppm), bis(diphenylphosphino)amine (dppa), and 1,1,1-tris(diphenylphosphinomethyl)ethane, as well as *N*-heterocyclic carbenes.[7,8]

Recently we have synthesized di- and tetranuclear copper hydride complexes [Cu$_2$(μ–H)(*meso*–**L**^{1})$_2$]$^+$ (**1**) and [Cu$_4$(μ_4–H)(μ–H)$_2$(*meso*–**L**^{1})$_2$]$^+$ supported by a linear tetraphosphine ligand (*n* = 1: **L**^{1} = dpmppm) (Figure 1), that showed facile reactivity toward CO$_2$ to give formate-bridged complexes via insertion of CO$_2$ into the Cu$_2$(μ–H) unit.[9] In contrast, similar syntheses using those with different central methylene chains and configurations at the inner P atoms (*n* = 2: *meso*– and *rac*–**L**^{2} (dpmppe), 3: *meso*–**L**^{3} (dpmppp)) afforded tri- and tetranuclear copper hydride complexes **2**–**5**, which were entirely inert against CO$_2$.[10] These results strongly suggested that the structures and reactivity of multinuclear copper hydride complexes could be tuned by varying the multidentate phosphine ligands.

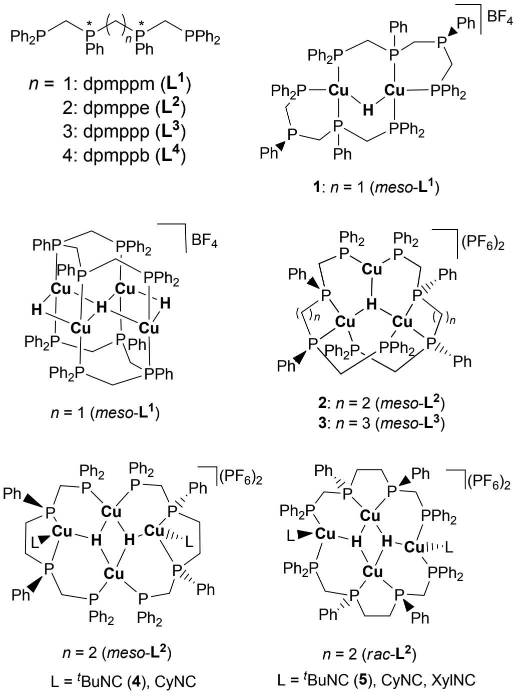

Figure 1. Structures of tetradentate phosphine ligands **L**$^{1-4}$ and copper hydride complexes **1**–**5**.

In the present study, we have utilized a new tetradentate phosphine ligand, *meso*–**L**^{4} (*n* = 4, dpmppb) (Figure 1) to elucidate its effects on the structures and reactivity of copper hydride complexes, and synthesized hexanuclear Cu–H complexes that catalyze a facile decomposition of FA into H$_2$ and CO$_2$. After optimizing catalytic conditions, an unsymmetric dinuclear copper motif bridged by the tetraphosphine was proposed as an active species.

Reaction of *meso*–L^4 with CuCl and RNC in the presence of $NaBH_4$ and NH_4PF_6 afforded colorless crystals of $[Cu_6(\mu_3–H)_2(meso–L^4)_3(RNC)_4](PF_6)_4$ (R = ^{t}Bu (**6a**), Cy (**6b**)) (Figure 2). The crystal structures of **6a**,**b** (Figures 2b, S1, and S2) were essentially similar to consist of two trinuclear copper units, $\{Cu_3(\mu_3–H)(meso–L^4)(RNC)_2\}^{2+}$, connected by one *meso*–L^4 with crystallographically imposed inversion center. Each Cu_3 unit is bridged by a μ_3–hydride to result in distorted triangular cores, unlike the isosceles triangles of **2** and **3** with *meso*–$L^{2,3}$ (Figure 1).

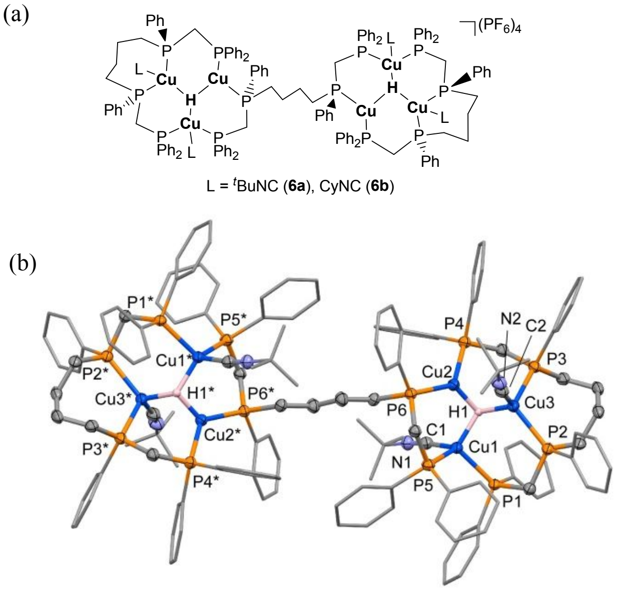

Figure 2. (a) Schematic structure of **6a** and **6b**. (b) Perspective view for the complex cation of **6a**.

Complex **6a** reacted gradually with CO_2 (1 atm) at r.t. in CD_3CN, and after 30 h, the hydride peak at –0.22 ppm for **6a** in ^1H NMR spectra diminished and a characteristic signal for a formate complex **7a** appeared at 8.85 ppm (Scheme 1). When the solution containing **7a** was stored under N_2 for 30 h, **6a** was regenerated (Figure S16). Treatment of **7a** with HBF_4 afforded FA quantitatively (Scheme 1). In light of the stoichiometric reactions, those of **6a** with FA were investigated to explore catalytic activity for FA decomposition. Reaction of **6a** with ca. 50 eq. of FA in CD_3CN for 20 h afforded **7a** quantitatively with formation of H_2 and CO_2, which were confirmed by GC and $^1H/^{13}C$ NMR techniques. After 60 h, all FA was consumed and **6a** was recovered in ~50% yield as a mixture with **7a** (Figure S17). The ESI–MS spectra of the reaction mixture showed a mono-cation peak at *m/z* 843.098 corresponding to $\{Cu_2(O_2CH)(meso–L^4)\}^+$. Complex **7a** is thus assumed an unsymmetric dinuclear copper formate complex of $[Cu_2(\mu–O_2CH)(meso–L^4)L_2]PF_6$ (L = ^{t}BuNC or CH_3CN) (Scheme 1), which is consistent with the $^1H\{^{31}P\}$ NMR spectra of the reaction mixture (Figure S17(c)). The bridging mode of the formate, κ*O,O'* or κ*O*, was not determined. It should be noted that O'Hair et al. recently reported gas-phase catalytic decomposition of FA, in which bimetallic $[MM'(\mu–H)(\mu–dppm)]^+$ (M, M' = Cu, Ag, Au) were estimated as active species on the basis of MS experiments and DFT calculations.[3]

Since **6a** showed the catalytic activity for FA dehydrogenation, those of related copper hydride complexes such as **1**–**6**, $[Cu_6H_6(PPh_3)_6]$, $[Cu_8H_6(dppm)_5](PF_6)_2$, and $[Cu_3H(O_2CH)(dppm)_3]PF_6$ [8] were investigated at 45 °C in CD_3CN for 3 h, and surprisingly, only **6** showed remarkable activity (Table S6). Addition of NEt_3 (40 mol% vs FA) enhanced catalytic activity, and increasing temperature to 70 °C led to the best result with **6** (conv. 100%), while **4** and **5** also showed moderate activities (conv. 48 and 66%) (Table S7).

Scheme 1. Reactions of **6a** with CO_2 or HCO_2H.

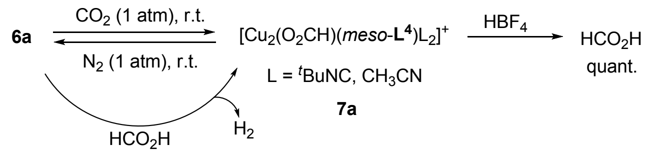

Several efforts were made to synthesize dinuclear copper complexes supported by tetradentate phosphine ligands L^n similar to **7a**. Reaction of *meso*–L^3 with $[Cu(CH_3CN)_4]PF_6$ in CH_3CN afforded $[Cu_2(meso–L^3)(CH_3CN)_3](PF_6)_2$ (**8**) (Figure S3), which possesses a cradle-type unsymmetric dinuclear scaffold with Cu···Cu = 3.3830(7) Å. Although **8** itself showed poor activity (conv. 9%) for FA decomposition, addition of ^{t}BuNC (2 eq.) to **8** increased the catalytic activity drastically (conv. 100%) (Table S8), demonstrating that ^{t}BuNC is indispensable to active species which are likely formulated as $[Cu_2(\mu–O_2CH)(meso–L^n)(^tBuNC)_2]PF_6$ (*n* = 3, 4).

Table 1. FA Dehydrogenation with Various Phosphine Ligands[a]

$$HCO_2H \xrightarrow[70\ ^oC,\ 3\ h,\ CD_3CN]{\substack{[Cu(CH_3CN)_4]PF_6 \\ \text{Phosphine ligands} \\ ^tBuNC\ (1.0\ eq.\ vs\ Cu) \\ NEt_3\ (0.4\ eq.\ vs\ FA)}} H_2 + CO_2$$

entry	Ligand[b]	Conv. (%)	TON (Cu mol^{-1})	TOF (h^{-1}·Cu mol^{-1})
1	0.5 *meso*–L^1	7	5.3×10	1.8×10
2	0.5 *rac*–L^1	0	0	0
3	0.5 *meso*–L^2	49	3.7×10^2	1.2×10^2
4	0.5 *rac*–L^2	62	4.7×10^2	1.6×10^2
5	0.5 *meso*–L^3	85	6.4×10^2	2.1×10^2
6	0.5 *rac*–L^3	28	2.1×10^2	7.0×10
7	0.5 *meso*–L^4	95	7.2×10^2	2.4×10^2
8	2 PPh_3	9	6.8×10	2.3×10
9	1 dppm[c]	63	4.7×10^2	1.8×10^2
10	1 dppe[c]	22	1.7×10^2	5.5×10
11	1 dppp[c]	4	3.0×10	1.0×10
12	1 dppb[c]	15	1.1×10^2	3.8×10

[a] To a NMR tube were added $[Cu(CH_3CN)_4]PF_6$ (1.3 mg, 3.4 μmol), phosphine (6.8 μmol of P), CD_3CN (0.45 mL), ^{t}BuNC (0.30 mg, 3.6 μmol), $MeNO_2$ for internal standard (5.6 mg, 92 mmol), NEt_3 (97 mg, 0.96 mmol), and HCO_2H (114 mg, 2.5 mmol, 7.5×10^2 eq. vs Cu). The mixture was heated at 70 °C for 3 h. The conversion (%), TON (Cu mol^{-1}), and TOF (h^{-1} Cu mol^{-1}) were calculated by using internal standard method of ^1H NMR measurement. [b] The number before the abbreviation indicates equivalent amounts for Cu to adjust Cu:P ratio to 1:2. [c] $Ph_2P(CH_2)_nPPh_2$ (n = 1: dppm, 2: dppe, 3: dppp, 4: dppb).

To evaluate the effect of phosphine ligands on the FA dehydrogenation, several phosphines were also examined (Table 1). The phosphines were mixed in an appropriate ratio with $[Cu(CH_3CN)_4]PF_6$ in the presence of ^{t}BuNC with a hope of generating the dinuclear active species like $[Cu_2(\mu–O_2CH)(meso–L^{3,4})(^tBuNC)_2]PF_6$ in situ. Among tetradentate phosphines L^n (*n* = 1–4), catalytic activities are higher in an order of *meso*–L^4 > *meso*–L^3 > *rac*–L^2 > *meso*–L^2 > *rac*–L^3 >> *meso*–L^1 >> *rac*–L^1. Monophosphine such as PPh_3 was not effective and among bidentate phosphines, dppm showed a moderate activity (conv. 63%) compared with dppe, dppp, and dppb, which may indicate preferential formation of dinuclear copper complex in the case of dppm.[11] Among other isocyanides, CyNC gave an excellent effect comparable to that of ^{t}BuNC (Tables S11,S12). These results strongly suggested that unsymmetric dinuclear copper species supported by the tetraphosphine and isocyanides are essential for the effective catalysts. The present catalytic system could be carried out in a large scale with a usual flask (FA/Cu = 5 x 10^3), the activity of which was monitored by volume of generated H_2 and CO_2 gases,[12] and the best performance with **8** in the presence of ^{t}BuNC (2 eq.) and NEt_3 (0.4 eq vs. FA) at 70 ºC for 8 h reached TON = 1.5 x 10^3 per Cu without obvious decomposition of the active species generated in situ (Figure S23), which is in accord with the results of recycling experiments with **6a** (see SI).

Scheme 2. Possible reaction mechanism for FA dehydrogenation.

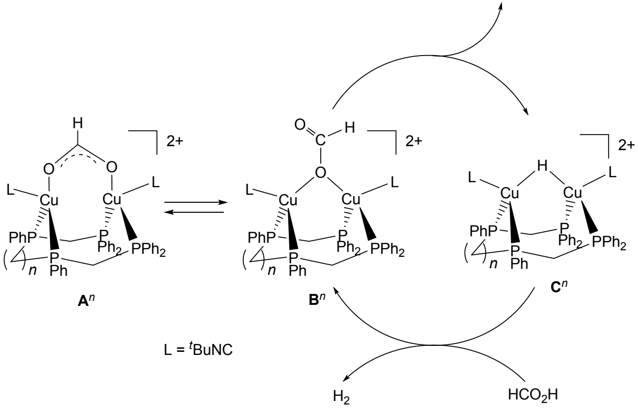

Based on the results of catalytic reactions, a possible reaction mechanism is proposed in Scheme 2. The formate complex $[Cu_2(\mu–O_2CH–\kappa O,O')(\mu–\mathbf{L}^n)(^tBuNC)_2]^+$ ($\mathbf{A}^n$, n = 2–4) might be generated under the reaction conditions and structural change of the formate ligand is likely to occur from κ*O,O'*–bridging mode to κ*O*–bridging to form $[Cu_2(\mu–O_2CH–\kappa O)(\mu–\mathbf{L}^n)(^tBuNC)_2]^+$ ($\mathbf{B}^n$) due to coordination of bulky isocyanide ligand (^{t}BuCN), which is supported by DFT calculations (vide infra). Since any hydride species were not detected in the catalytic reaction conditions, decarboxylation of $\mathbf{B}^n$ to give a μ–hydride complex, $[Cu_2(\mu–H)(\mu–\mathbf{L}^n)(^tBuNC)_2]^+$ ($\mathbf{C}^n$), is estimated as rate-determining step, and $\mathbf{C}^n$ readily reacts with FA, generating $\mathbf{B}^n$ and H_2, to complete the catalytic cycle. The assumption is consistent with a small primary deuterium kinetic isotope effect (KIE) of 2.98(2) derived from the catalytic decomposition of DCOOH (see SI, Figure S25).[13]

In order to confirm the proposed mechanism, theoretical calculations with DFT methods were carried out on a model system with *meso*–$\mathbf{L}^3$, including $[Cu_2(\mu–O_2CH–\kappa O,O')(meso–\mathbf{L}^3)(^tBuNC)_2]^+$ ($\mathbf{A}^3$), $[Cu_2(\mu–O_2CH–\kappa O)(meso–\mathbf{L}^3)(^tBuNC)_2]^+$ ($\mathbf{B}^3$), and $[Cu_2(\mu–H)(meso–\mathbf{L}^3)(^tBuNC)_2]^+$ ($\mathbf{C}^3$) (Figures 3 and S26). Due to repulsive interaction with bulky ^{t}BuNC ligands, the formate–κ*O* bridged structure $\mathbf{B}^3$ (Cu···Cu = 3.503 Å) is appreciably stable by Δ*G*º −3.3 kcal/mol in comparison with the formate–κ*O,O'* bridged structure $\mathbf{A}^3$ (Cu···Cu = 3.909 Å), and is thus estimated to be involved in the catalytic cycle. The μ–H structure of $\mathbf{C}^3$ is also identified with appropriate metric parameters (Cu···Cu = 2.773 Å), which are comparable to those of **1**[8] (Figures S26 and S27). These results revealed that the κ^2,κ^2–bridging mode of *meso*–$\mathbf{L}^3$, entirely close to that of **8**, can accommodate the unsymmetric dicopper centers flexibly to promote the decomposition. The difference of Gibbs free energy between $\mathbf{B}^3$ and $\mathbf{C}^3$ + CO_2 is +8.7 kcal/mol, indicating an endothermic process for the decarboxylation, and the H_2 generation step from $\mathbf{C}^3$ + HCO_2H to $\mathbf{B}^3$ + H_2 is exothermic with Δ*G*º −17.6 kcal/mol probably with low energy barriers.

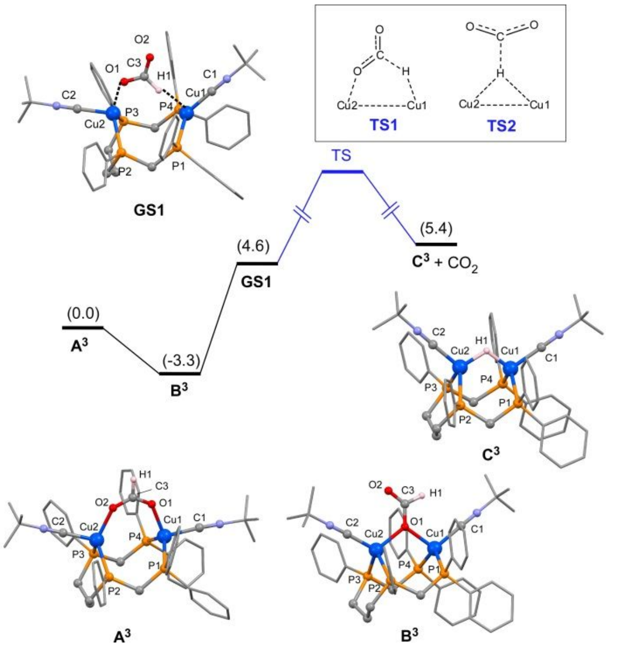

Figure 3. DFT optimized structures of $\mathbf{A}^3$, $\mathbf{B}^3$, $\mathbf{C}^3$, and **GS1**, and simplified Gibbs free-energy profiles. Numerical values in parentheses are difference in G^o_{298} relative to $\mathbf{A}^3$ in kcal mol^{-1}. Estimated transition states, **TS1** and **TS2**, for decarboxylation of **GS1** to give $\mathbf{C}^3$.

As to the rate-determining step, we have tried to find a transition state (TS) from $\mathbf{B}^3$ to $\mathbf{C}^3$, and at first, obtained a high energy ground state (**GS1**) that involves a loosely trapped formate in κ*O,H*–fashion before C–H cleavage reaction (Figures 3 and S26d). DFT calculations were performed to find a transition state between **GS1** and $\mathbf{C}^3$, but reliable structures were not obtained presumably due to shallow potentials. Nevertheless, on the basis of **GS1**, two transition states, **TS1** and **TS2**, could be envisaged for C–H bond cleavage of the formate (Figure 3). A hydride abstraction proceeds on one Cu side with anchoring O atom to another Cu center in **TS1**, and this type of mechanism was proposed by O'Hair et al. for the gas-phase FA dehydrogenation.[3a] Alternatively, a hydride abstraction is promoted on the both Cu centers with μ–H bridging fashion in **TS2**, which is reminiscent of the transition state estimated for insertion of CO_2 into $Cu_2(\mu–H)$ unit of **1**.[8] The present DFT calculations do not determine the exact reaction mechanism, but demonstrate that synergistic effects of the unsymmetric Cu_2 unit play important role for the hydride abstraction; stabilization of the hydride species as the $Cu_2(\mu–H)$ form might be a driving force of β-hydride elimination.

In conclusion, a new linear tetraphosphine, *meso*–$Ph_2PCH_2P(Ph)(CH_2)_4P(Ph)CH_2PPh_2$ (*meso*–$\mathbf{L}^4$) was synthesized and utilized to create hexanuclear copper hydride complexes, $[Cu_6(\mu_3–H)_2(meso–\mathbf{L}^4)_3(RNC)_4](PF_6)_4$ (R = ^{t}Bu, Cy), that were found to catalyze a facile decomposition of FA into H_2 and CO_2. After optimizing catalytic conditions, an unsymmetric dinuclear copper motif bridged by *meso*–$\mathbf{L}^{3,4}$, $[Cu_2(meso–\mathbf{L}^{3,4})(^tBuNC)_2]^{2+}$, was proposed as an active species to promote the FA decomposition by virtue of synergistic effects of the Cu_2 scaffold. The present system is the first viable catalytic dehydrogenation of FA by using cheap base metallic Cu complexes.

ASSOCIATED CONTENT

Supporting Information

The Supporting Information is available free of charge on the ACS Publications website at DOI: 10.1021/jacs.9b#####. Experimental procedure, NMR and ESI mass spectra, Tables for catalytic FA decomposition, DFT optimized structures (PDF). Crystallographic data for **6a,b** and **8**.

AUTHOR INFORMATION

Corresponding Authors

*t.nakajima@cc.nara-wu.ac.jp
*tanase@cc.nara-wu.ac.jp

ORCID

Takayuki Nakajima: 0000-0003-3884-9205
Kanako Nakamae: 0000-0002-4256-9305
Yasuyuki Ura: 0000-0003-0484-1299
Tomoaki Tanase: 0000-0003-1838-0112

Notes

The authors declare no competing financial interests.

ACKNOWLEDGMENT

This work was supported by a Grant-in-Aid for Scientific Research (no. 18H03914) and on Priority Area 2107 (no. 22108521, 24108727) and 2802 (no. 17H05374, 19H04582) from the Ministry of Education, Culture, Sports, Science and Technology, Japan. The computations were performed using Research Center for Computational Science, Okazaki, Japan. The authors thank Prof. Kohtaro Osakada of Tokyo Institute of Technology for help in MS spectral measurements.

REFERENCES

(1) For recent review, see: (a) Sordakis, K.; Tang, C.; Vogt, L. K.; Junge, H.; Dyson, P. J.; Beller, M.; Laurenczy, G. Homogeneous Catalysis for Sustainable Hydrogen Storage in Formic Acid and Alcohols. *Chem. Rev.* **2018**, *118*, 372. (b) Onishi, N.; Laurenczy, G.; Beller, M.; Himeda, Y. Recent progress for reversible homogeneous catalytic hydrogen storage in formic acid and in methanol. *Coord. Chem. Rev.* **2018**, *373*, 317. (c) Mellmann, D.; Sponholz, P.; Junge, H.; Beller, M. Formic Acid as a Hydrogen Storage Material–Development of Homogeneous Catalysts for Selective Hydrogen Release. *Chem. Soc. Rev.* **2016**, *45*, 3954. (d) Wang, W.-H.; Himeda, Y.; Muckerman, J. T.; Manbeck, G. F.; Fujita, E. CO_2 Hydrogenation to Formate and Methanol as an Alternative to Photo- and Electrochemical CO_2 Reduction. *Chem. Rev.* **2015**, *115*, 12936.

(2) Scotti, N.; Psaro, R.; Ravasio, N.; Zaccheria, F. A New Cu-based System for Formic Acid Dehydrogenation. *RSC Adv.* **2014**, *4*, 61514.

(3) (a) Zavras, A.; Krstić, M.; Dugourd, P.; Bonačić-Koutecký, V.; O'Hair, R. A. Selectivity Effects in Bimetallic Catalysis: Role of the Metal Sites in the Decomposition of Formic Acid into H_2 and CO_2 by the Coinage Metal Binuclear Complexes $[dppmMM'(H)]^+$. *ChemCatChem* **2017**, *9*, 1298. (b) Krstić, M.; Jin, Q.; Khairallah, G. N.; O'Hair, R. A.; Bonačić-Koutecký, V. How to Translate the $[LCu_2(H)]^+$-Catalysed Selective Decomposition of Formic Acid into H_2 and CO_2 from the Gas Phase into a Zeolite. *ChemCatChem* **2018**, *10*, 1173.

(4) For recent review, see: (a) Deutsch, C.; Krause, K.; Lipshutz, B. H. CuH-Catalyzed Reactions. *Chem. Rev.* **2008**, *108*, 2916. (b) Dhayal, R. S.; van Zyl, W. E.; Liu, C. Polyhydride Copper Clusters: Synthetic Advances, Structural Diversity, and Nanocluster-to-Nanoparticle Conversion. *Acc. Chem. Res.* **2016**, *49*, 86. (c) Riant, O. Copper(I) hydride reagents and catalysts, in The Chemistry of Organocopper Compounds. Z. Rappoport, I. Marek, Eds., John Wiley & Sons, West Sussex, England, **2009**, p. 731. (d) Jordan, A. J.; Lalic, G.; Sadighi, J. P. Coinage Metal Hydrides: Synthesis, Characterization, and Reactivity. *Chem. Rev.* **2016**, *116*. 8318.

(5) (a) Motokura, K.; Kashiwame, D.; Takahashi, N.; Miyaji, A.; Baba, T. Highly Active and Selective Catalysis of Copper Diphosphine Complexes for the Transformation of Carbon Dioxide into Silyl Formate. *Chem. Eur. J.* **2013**, *19*, 10030. (b) Zhang, L.; Cheng, J.; Hou, Z. Highly efficient catalytic hydrosilylation of carbon dioxide by an N-heterocyclic carbene copper catalyst. *Chem. Commun.* **2013**, *49*, 4782. (c) Shintani, R.; Nozaki, K. Copper-Catalyzed Hydroboration of Carbon Dioxide. *Organometallics* **2013**, *32*, 2459. (d) Zall, C. M.; Linehan, J. C.; Appel, A. M. Triphosphine-Ligated Copper Hydrides for CO_2 Hydrogenation: Structure, Reactivity, and Thermodynamic Studies. *J. Am. Chem. Soc.* **2016**, *138*, 9968. (e) Jordan, A. J.; Wyss, C. M.; Bacsa, J.; Sadighi, J. P. Synthesis and Reactivity of New Copper(I) Hydride Dimers. *Organometallics* **2006**, *35*, 613. (f) Zall, C. M.; Linehan, J. C.; Appel, A. M. A Molecular Copper Catalyst for Hydrogenation of CO_2 to Formate. *ACS Catal.* **2015**, *5*, 5301. (g) Watari, R.; Kayaki, Y.; Hirano, S.; Matsumoto, N.; Ikariya, T. Hydrogenation of Carbon Dioxide to Formate Catalyzed by a Copper/1,8-Diazabicyclo[5.4.0]undec-7-ene System. Watari, R.; Kayaki, Y.; Hirano, S.; Matsumoto, N.; Ikariya, T.; *Adv. Synth. Catal.* **2015**, *357*, 1369.

(6) (a) Churchill, M. R.; Bezman, S. A.; Osborn, J. A.; Wordmald, J. Synthesis and Molecular Geometry of Hexameric Triphenylphosphinocopper(1) Hydride and the Crystal Structure of $H_6Cu_6(PPh_3)_6$ HCONMe. *Inorg. Chem.* **1972**, *11*, 1818. (b) Stevens, R. C.; McLean, M. R.; Bau, R. Neutron Diffraction Structure Analysis of a Hexanuclear Copper Hydride Complex, $H_6Cu_6[P(p\text{-tolyl})_3]_6$: An Unexpected Finding. *J. Am. Chem. Soc.* **1989**, *111*, 3472. (c) Goeden, G. V.; Caulton, K. G. Soluble Copper Hydrides: Solution Behavior and Reactions Related to CO Hydrogenation. *J. Am. Chem. Soc.* **1981**, *103*, 7354. (d) Lemmen. T. H.; Folting, K.; Huffman, J. C.; Caulton, K. G. Copper Polyhydrides. *J. Am. Chem. Soc.* **1985**, *107*, 7774. (e) Albert, C. F.; Healy, P. C.; Kildea, J. D.; Raston, C. L.; Skelton, B. W.; White, A. H. Lewis-Base Adducts of Group 11 Metal(1) Compounds. 49. Structural Characterization of Hexameric and Pentameric (Tripheny1phosphine)copper (I) Hydrides. *Inorg. Chem.* **1989**, *28*, 1300. (f) Eberhart, M. S.; Norton, J. R.; Zuzek, A.; Sattler, W.; Ruccolo, S. Electron Transfer from Hexameric Copper Hydrides. *J. Am. Chem. Soc.* **2013**, *135*, 17262. (g) Nguyen, T.-A. D.; Goldsmith, B. R.; Zaman, H. T.; Wu, G.; Peters, B.; Hayton, T. W. Synthesis and Characterization of a Cu_{14} Hydride Cluster Supported by Neutral Donor Ligands. *Chem. Eur. J.* **2015**, *21*, 5341. (h) Nguyen, T.-A. D.; Jones, Z. R.; Goldsmith, B. R.; Buratto, W. R.; Wu, G.; Scott, S. L.; Hayton, T. W. A Cu_{25} Nanocluster with Partial Cu(0) Character. *J. Am. Chem. Soc.* **2015**, *137*, 13319.

(7) (a) Jordan, A. J.; Lalic, G.; Sadighi, J. P. Coinage Metal Hydrides: Synthesis, Characterization, and Reactivity. *Chem. Rev.* **2016**, *116*, 8318. (b) Dhayal, R. S.; van Zyl, W. E.; Liu, C. W. Copper hydride clusters in energy storage and conversion. *Dalton Trans,* **2019**, *48*, 3531. (c) Cook, A. W.; Nguyen, T.-A. D.; Buratto, W. R.; Wu, G.; Hayton, T. W. Synthesis, Characterization, and Reactivity of the Group 11 Hydride Clusters $[Ag_6H_4(dppm)_4(OAc)_2]$ and $[Cu_3H(dppm)_3(OAc)_2]$. *Inorg. Chem.* **2016**, *55*, 12435. (d) Mao, Z.; Huang, J.-S.; Che, C.-M.; Zhu, N.; Leung, S. K.-Y.; Zhou, Z.-Y. Unexpected Reactivities of Cu_2(diphosphine)$_2$ Complexes in Alcohol: Isolation, X-ray Crystal Structure, and Photoluminescent Properties of a Remarkably Stable $[Cu_3(\text{diphosphine})_3(\mu_3\text{–H})]^{2+}$ Hydride Complex. *J. Am. Chem. Soc.* **2005**, *127*, 4562. (e) Li, J.; White, J. M.; Mulder, R. J.; Reid, G. E.; Donnelly, P. S.; O'Hair, R. A. J. Synthesis, Structural Characterization, and Gas-Phase Unimolecular Reactivity of Bis(diphenylphosphino)amino Copper Hydride Nanoclusters $[Cu_3(X)(\mu_3\text{–H})((PPh_2)_2NH)_3](BF_4)$, Where X = μ_2–Cl and μ_3–BH_4. *Inorg. Chem.* **2016**, *55*, 9858. (f) Ma, H. Z.; Li, J.; Canty, A. J.; O'Hair, R. A. J. Cluster transformation of $[Cu_3(\mu_3\text{–H})(\mu_3\text{–}BH_4)((PPh_2)_2NH)_3](BF_4)$ to $[Cu_3(\mu_3\text{–H})(\mu_2,\mu_1\text{–}S_2CH)((PPh_2)_2NH)_3](BF_4)$ via reaction with CS_2. X-ray structural characterization and reactivity of cationic clusters explored by multistage mass spectrometry and computational studies. *Dalton Trans.* **2017**, *46*, 14995.

(8) Nakamae, K.; Tanaka, M.; Kure, B.; Nakajima, T.; Ura, Y.; Tanase, T. A Fluxional Cu_8H_6 Cluster Supported by Bis(diphenylphosphino)methane and Its Facile Reaction with CO_2. *Chem. Eur. J.* **2017**, *23*, 9457.

(9) Nakamae, K.; Kure, B.; Nakajima, T.; Ura, Y.; Tanase, T. Facile Insertion of Carbon Dioxide into $Cu_2(\mu\text{–H})$ Dinuclear Units Supported by Tetraphosphine Ligands. *Chem. Asian J.* **2014**, *9*, 3106-3110.

(10) Nakajima, T.; Kamiryo, Y.; Hachiken, K.; Nakamae, K.; Ura, Y.; Tanase, T. Tri- and Tetranuclear Copper Hydride Complexes Supported by Tetradentate Phosphine Ligands. *Inorg. Chem.* **2018**, *57*, 11005.

(11) Harvey, P. D.; Drouin, M.; Zhang, T. Crystallographic, Theoretical, and Spectroscopic Studies of the Luminescent d^{10}–d^{10} Binuclear Copper Acetate Complex $Cu_2(dppm)_2(O_2CCH_3)^+$. *Inorg. Chem*. **1997**, *36*, 4998.

(12) Wang, Z.;Lu, S.-M.; Li, J.; Wang, J.; Li, C. Unprecedentedly High Formic Acid Dehydrogenation Activity on an Iridium Complex with an N,N'-Diimine Ligand in Water. *Chem. Eur. J.* **2015**, *21*, 12592.

(13) (a) Boddien, A.; Mellmann, D.; Gärtner, F.; Jackstell, R.; Junge, H.; Dyson, P. J.; Laurenczy, G.; Ludwig, R.; Beller M. Efficient Dehydrogenation of Formic Acid Using an Iron Catalyst. *Science* **2011**, *333*, 1733. (b) Wang, W.-H.; Xu, S.; Manaka, Y.; Suna, Y.; Kambayashi, H.; Muckerman, J. T.; Fujita, E.; Himeda, Y. Formic Acid Dehydrogenation with Bioinspired Iridium Complexes: A Kinetic Isotope Effect Study and Mechanistic Insight. *ChemSusChem* **2014**, *7*, 1976.

For the use of Graphical Abstract